2018 26th Mediterranean Conference on Control and Automation (MED)
Zadar, Croatia, June 19-22, 2018

Distributed state feedback control for aeroelastic morphing wing flutter supression

Filip Svoboda[1] and Martin Hromčík[2] and Kristian Hengster–Movric[3]

Abstract— **This paper offers a novel approach at flutter suppression problem on morphing wing and relates to current research of morphing aircraft. The active flutter suppression task is formulated as a state synchronization in a network of identical Linear Time-Invariant (LTI) systems. These systems consist of wing segments which can be actuated separately. Finite Element Method (FEM) approach and unsteady aerodynamics represented by Theodorsen function are used for flexible morphing wing modeling. An example of distributed Linear–Quadratic Regulator (LQR) state synchronization is shown in this paper. Comparison in time-domain, frequency-domain, and flutter speeds has been done for the system with distributed LQR and the original system.**

I. INTRODUCTION

Flutter is the most important of all aeroelastic phenomena causing unstable self-excited vibrations [1]. This instability occurs above the critical (flutter) speed where at least one of the modes is no longer damped. Flutter can take various forms involving different interacting modes and often leads to catastrophic structural failure. Reduction of structural weight to maximize efficiency and agility for modern aircraft also reduces stiffness and thereby increases the likelihood of flutter. One possible solution is active flutter suppression using information from sensors to compute control surface action and avoid flutter.

This paper is focused on active flutter suppression of a morphing wing. Morphing wing represents a new concept of an aircraft wing changing its external shape during flight. Recent research in this area [2], [3] shows a large number of benefits such as better efficiency, aerodynamic noise reduction, mass reduction, etc. Mechanical construction uses smart materials such as shape memory alloys (SMA), shape memory polymers (SMP) or piezoelectric actuators [4] to reshape a wing geometry. Morphing wings are no longer a matter of purely theoretical considerations. An example is an aircraft with "Mission Adaptive Compliant Wing" developed by FlexSys Inc. [5]. These new aircraft actuation possibilities also motivate novel approaches to control design of active damping and flutter suppression systems, which we believe are thus far not commonly used in the field of aircraft control systems thus far. Especially interesting for this purpose are the distributed and cooperative control concepts dealing with a problem of controlling a multi-agent system [6], where multiple dynamic entities share information to accomplish a common goal.

In this work, we formulate flutter suppression as a cooperative tracking control problem, [7] also known as pinning control or synchronization to leader [8],[9]. The control law is based on local rules applied to agents in a system and uses an average of its information and information from neighbors or the leader. In case of the morphing wing the wing is composed of a finite number of segments, and its dynamics are described by states in individual nodes between the segments. States of these nodes should be synchronized with the leader, which is fuselage. Several pinning strategies are shown below.

Three–dimensional wing model [10] is presented, where finite element method allows precise structural description along the wingspan. It provides information about bend, heave, and torsion at several points. For unsteady aerodynamics, modeling, one can use the high–fidelity Computational Fluid Dynamics (CFD) approach [11],[12] with a very high number of states or the panel methods derived from the potential theory. The most widely used panel method for unsteady aerodynamics is the doublet lattice method (DLM) [13]. Steady part of DLM can be replaced by steady vortex lattice method (VLM) [14]. These methods provide the aerodynamic force distribution on the aerodynamic grid. The resulting aeroelastic model is composed of aerodynamic and structural parts. This model is inappropriate for cooperative control purposes due to its complexity and complicated structure. Therefore, we construct the model with the abovestated cooperative control design intentions in mind. The resulting model features good modeling accuracy and captures the 3D nature of the problem – as opposed to standard 2D aeroelastic models often used so far [15]. At the same time, it has to be of manageable complexity – compared to complex 3D models relying on the panel methods or the CFD solvers for aerodynamics calculations. It therefore appears, we believe, as most suitable for the design of distributed control laws for the near-future morphing wing concepts and similar applications with a large number of actuators.

The paper is organized as follows. The aeroelastic wing model is developed in Section II. We explain our motivation and discuss the structure of the model. Section III. is devoted to cooperative control, where we formulate flutter

This work was supported by the Czech Republic Granting Agency grant No. 16-21961S, by the Czech Republic Granting Agency, junior grant No. 16-25493Y and by the Grant Agency of the Czech Technical University in Prague, grant No. SGS16/232/OHK3/3T/13.

[1]Filip Svoboda is with Faculty of Electrical Engineering, Czech Technical University in Pragu, Karlovo náměstí 13/E, 12135 Prague, Czech Republic svobofi2@fel.cvut.cz

[2]Martin Hromčík with Faculty of Electrical Engineering, Czech Technical University in Pragu, Karlovo náměstí 13/E, 12135 Prague, Czech Republic xhromcik@fel.cvut.cz

[3]Kristian Hengster–Movric with Faculty of Electrical Engineering, Czech Technical University in Pragu, Karlovo náměstí 13/E, 12135 Prague, Czech Republic hengskri@fel.cvut.cz

suppression task as a cooperative state variable feedback. Examples of controllers with frequency-domain and time-domain analysis are presented in Section IV. Concluding remarks are presented in section V.

II. Aeroelastic morphing wing model

The model we propose has two mutually interconnected parts. The first one represents the mechanical structure while the second one models the aerodynamics. These parts form each wing segment model and the entire wing is composed of these segments.

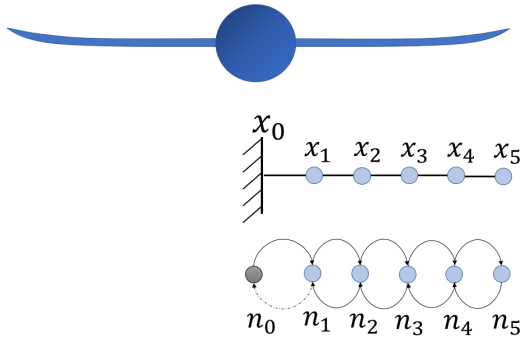

Fig. 1. Wing representation - FEM and graph structure

Figur 1 shows an aircraft, where the wing is divided into five sections with states x_i, corresponding to nodes i. These nodes can also be represented as agents n_i with their dynamics. Although agents dynamics and also graph representing the network between agents are given by mechanical properties of the wing, cooperative control can be used quite naturally with such a model to design a robust distributed controller to modify the whole wing dynamics and thus prevent flutter. In this setup, the node x_0 (fuselage) acts as the leader. Leader affects all agents and vice versa. This interaction depends on the position of the agent in the network through which the interaction is propagated. The effect of the leader propagates through the network, it being felt with different delays due to each agents location in the network. A cooperative controller can, of course, have a different network topology where information from the leader is directly made available to the most remote agent and thus, for instance, speed up the last nodes response. We can, for instance, artificially clamp the wing at various points and strengthen the structure artificially in this manner.

Structure of the model is essential for further use in cooperative control design where we require the possibility of the model decomposition to agents. This is the reason why we do not propose to use the complex 3D aeroelastic models and subsequent model reduction techniques. We would thereby lose the physical meaning of states belonging to the given part of the wing, (agent). In contrast, our model is composed of several structural and aerodynamic parts like in "strip" theory [15], where the wing is considered to be composed of a number of elemental chordwise "strips." All segments have the structural part and aerodynamic part in feedback.

This model assumes that the lift on each wing segment is the same as if that segment were part of an infinite span wing. Boundary effects (fringe effects) are thus disregarded. Hence, the presence of lift in the tip region implies a pressure discontinuity at the tip. This cannot occur in practice, where the spanwise lift distribution falls off to zero at the tip. The same lift distribution assumption is commonly used in practical flutter analysis. The total lift is found by integrating the effect on all the segments, and it is thus greater than for a real wing. Our proposed model is thus conservative and predicted model flutter speed is lower than it is in reality. It creates a certain margin for flutter analysis.

1) Mechanical structure: Finite element approach is used for mechanical structure modeling. This method is common in aircraft aeroelastic calculations, and it approximates the behavior of a continuous mechanical structure. It divides the structure into a number of "finite elements" interconnected at discrete points. In this case, each finite element is the Euler-Bernoulli beam with three degrees of freedom (band, heave, and twist), see Figure 2.

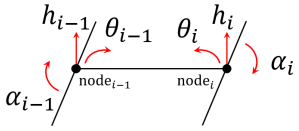

Fig. 2. Euler–Bernoully beam

A solution of Euler–Bernoulli beam equation (1) can be found as a linear combination of shape functions expressed as a cubic polynomial.

$$EI\frac{d^4u}{dx^4} = -f \tag{1}$$

For more complex problems where displacement and stress are varying more rapidly, more elements must be employed. Forces and torques may only be applied to the element nodes. The number of elements also determines the number of model wing modes. An example of mode shapes for a wing with five sections (five beams) is depicted in Figures 3 and 4.

Let the model considered further have five elements. It means six nodes including clamping to the fuselage. Equation of motion for entire system is (2), where M_w, C_w and K_w are the wing mass, damping and stiffness matrices, F_w is a generalized force vector, (node forces and torques). Mass and stiffness matrices are composed of element mass and stiffness matrices, given by (3) and (4), where m is mass per unit length, j is inertia per unit length, G is modulus of rigidity, E is elastic modulus, I_z is moment of area and L is a length of a beam. Damping matrix C_w is, in our case, a linear combination of M_w and K_w, (Rayleigh damping). Vector $X = \begin{bmatrix} v_0 & \theta_0 & \alpha_0 & v_1 & \theta_1 & \alpha_1 & \dots & v_N & \theta_N \alpha_N \end{bmatrix}^T$ contains displacement variables of each node. Structure of the

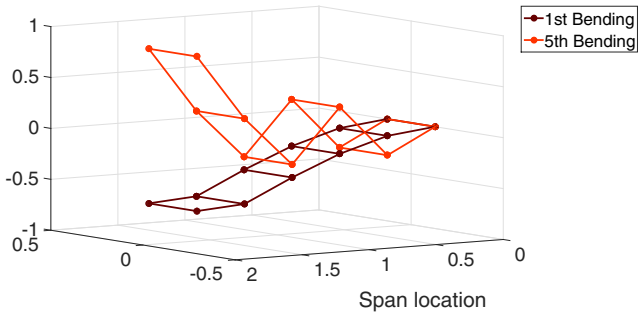

Fig. 3. First and fifth bending mode shape

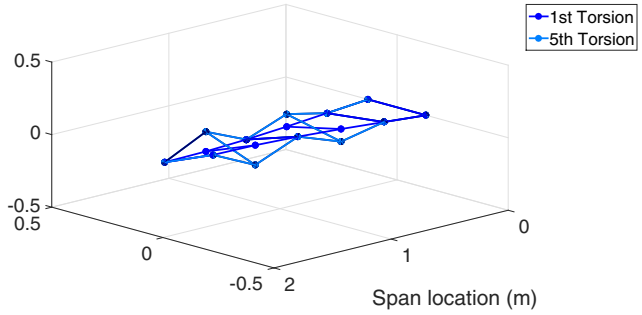

Fig. 4. First and fifth torsional mode shape

mass and stiffness matrices depends on the FEM structure. For structure in Figure 1 matrices K_w and M_w have element stiffness and element mass matrices as diagonal blocks shown in Figure 5. More details about FEM based model can be found in [15].

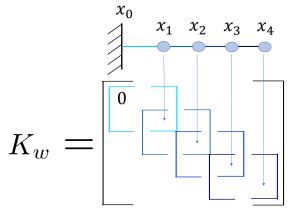

Fig. 5. Stiffness matrix structure with indicated k_e matrices

$$M_w\ddot{X} + C_w\dot{X} + K_wX = F_w \tag{2}$$

$$k_e = \begin{bmatrix} \frac{12EI_z}{L^3} & \frac{6EI_z}{L^3} & 0 & \frac{-12EI_z}{L^3} & \frac{6EI_z}{L^2} & 0 \\ \frac{6EI_z}{L^2} & \frac{4EI_z}{L} & 0 & \frac{-6EI_z}{L^2} & \frac{2EI_z}{L} & 0 \\ 0 & 0 & \frac{GJ_x}{L} & 0 & 0 & \frac{-GJ_x}{L} \\ \frac{-12EI_z}{L^3} & \frac{-6EI_z}{L^3} & 0 & \frac{12EI_z}{L^3} & \frac{-6EI_z}{L^2} & 0 \\ \frac{6EI_z}{L^2} & \frac{2EI_z}{L} & 0 & \frac{-6EI_z}{L^2} & \frac{4EI_z}{L} & 0 \\ 0 & 0 & \frac{-GJ_x}{L} & 0 & 0 & \frac{GJ_x}{L} \end{bmatrix} \tag{3}$$

$$m_e = \begin{bmatrix} \frac{156mL}{420} & \frac{22mL^2}{420} & 0 & \frac{54mL}{420} & \frac{-13mL^2}{420} & 0 \\ \frac{22mL^2}{420} & \frac{4mL^3}{420} & 0 & \frac{13L^2}{420} & \frac{3mL^3}{420} & 0 \\ 0 & 0 & \frac{jL}{3} & 0 & 0 & \frac{jL}{6} \\ \frac{54mL}{420} & \frac{13mL^2}{420} & 0 & \frac{156mL}{420} & \frac{-22mL^2}{420} & 0 \\ \frac{-13mL^2}{420} & \frac{-3mL^3}{420} & 0 & \frac{-22mL^2}{420} & \frac{4mL^3}{420} & 0 \\ 0 & 0 & \frac{jL}{6} & 0 & 0 & \frac{jL}{3} \end{bmatrix} \tag{4}$$

2) Aerodynamics: Second important part of aeroelastic wing model is the unsteady aerodynamics. Unsteady effects are an outcome of circulation changes around a moving airfoil. The resulting force and torque are functions of dynamic motions frequency. This relation is described in the time domain by Wagner function and in the frequency domain by Theodorsen function [16]. Amplitude attenuation and phase lag are functions of the dimensionless reduced frequency $k = \frac{\omega b}{V}$, where ω is airfoil oscillating frequency, b is a semi–chord, and V is speed. The classical solution for the lift and torque expressed per unit span is (5) and (6). Theodorsen function $C(k)$ is approximated by a complex function (7) for $k \leq 0.5$ and (8) for $k > 0.5$ [15]. Function $C(k)$ is practically a second order LTI filter and can be rewritten to the transfer function form $C(s)$ and used inside the aerodynamic block.

$$\begin{aligned} L = &-\rho b^2(\pi\ddot{h} - \pi ba\ddot{\alpha} + V\pi\dot{\alpha}) \\ &-2\pi\rho bC(k)[\dot{h} + b(\frac{1}{2} - a)\dot{\alpha} + V\alpha] \end{aligned} \tag{5}$$

$$\begin{aligned} M = &-\rho\pi b^2[ba\ddot{h} - Vb(\frac{1}{2} - a)\dot{\alpha} - b^2(\frac{1}{8} + a^2)\ddot{\alpha}] \\ &+2\pi\rho Vb^2(\frac{1}{2} + a)C(k)[\dot{h} + b(\frac{1}{2} - a)\dot{\alpha} + V\alpha] \end{aligned} \tag{6}$$

$$C(k) = 1 - \frac{0.165}{1 - \frac{0.045}{k}j} - \frac{0.335}{1 - \frac{0.30}{k}j}, \tag{7}$$

$$C(k) = 1 - \frac{0.165}{1 - \frac{0.041}{k}j} - \frac{0.335}{1 - \frac{0.32}{k}j}. \tag{8}$$

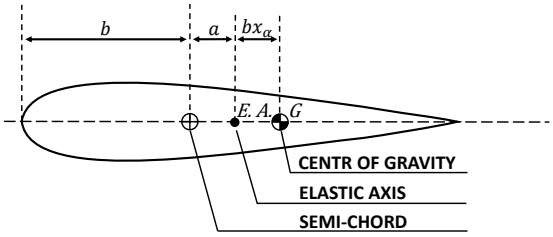

Fig. 6. Wing airfoil

III. Cooperative control

In this section, we assume the full state information is available, and design the cooperative state variable feedback control using linear quadratic regulator (LQR) design approach. The control law is described in (9), where u_i is i^{th} input to system, c is a scalar coupling gain, K is a control gain matrix and ϵ_i is neighborhood synchronization error of node i defined as (10). Neighborhood synchronization error for node i depends on local communication with their neighbors described by adjacency matrix $A = [a_{ij}]$ and also on communication with leader given by pinning matrix $G = diag(g_i)$. We will present control laws where each node has information from their neighbors (11) and some of them also from the leader.

$$u_i = cK\epsilon_i \tag{9}$$

$$\epsilon_i = \sum_{j \in N_i} a_{ij}(x_j - x_i) + g_i(x_0 - x_i) \tag{10}$$

$$A = [a_{ij}] = \begin{bmatrix} 0 & 1 & 0 & 0 & 0 \\ 1 & 0 & 1 & 0 & 0 \\ 0 & 1 & 0 & 1 & 0 \\ 0 & 0 & 1 & 0 & 1 \\ 0 & 0 & 0 & 1 & 0 \end{bmatrix} \tag{11}$$

Compared to centralized state feedback $K_{centralized}$ where the number of columns is equal to the number of states of the entire system, our control gain matrix K has a number of columns equal to the number of agents states S_{agent}. It is N-times less, where N is a number of agents.

A. LQR design

Design of control gain matrix K is based on single-agent dynamics. However, agents representing flexible wing already have coupling depicted in Figure 1. Therefore we approximated single agent dynamics as a node with fixed neighbors. Speed used for LQR design is $V_d = 1.2V_f$, where flutter speed of nominal system is $V_f = 118.54$, see Figure 7. This system with matrices (A_d, B_d, C_d, D_d) will be used for LQR design. We obtain control gain matrix K as (12), where P is positive definite solution of the algebraic Riccati equation (13). Sizes of matrices R and Q correspond to the number of inputs and number of states of a single agent. Consequently, controller tuning is much easier compared to centralized LQR.

$$K = R^{-1}B_dP \tag{12}$$

$$0 = A_d^TP + PA_d + Q - PB_dR^{-1}B_d^TP \tag{13}$$

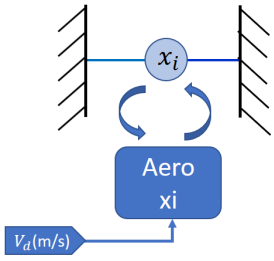

Fig. 7. Single-agent dynamics approximation

IV. Results

Examples of cooperative state feedback controllers will be presented in this section. We will show controllers damping capabilities and pinning position influence.

Our controller is designed independently of adjacency matrix A and pinning matrix G. Thus, we can show pinning to various nodes with the same K. Pinning to the farthest node from the fuselage is the best choice for one node pinning. We artificially clamp this node to the fuselage in this manner. Figure 8 shows flutter speeds with pinning to individual nodes. Of course, the higher flutter speed corresponds to all node pinning where the new flutter speed is 156 m/s. For the following analysis, we use pinning to node five (14) and channel from disturbance (additional torque at all nodes) to node five.

Controller designing methodology is not dependent on a number of wing segments; it means that the same control gain matrix K can be used for a system with a different number of the same segments. By extension of the wing with three more segments, the wings flutter speed decrease to 82.4 m/s. However, the flutter speed with cooperative LQR and same matrix K is 115.4 m/s.

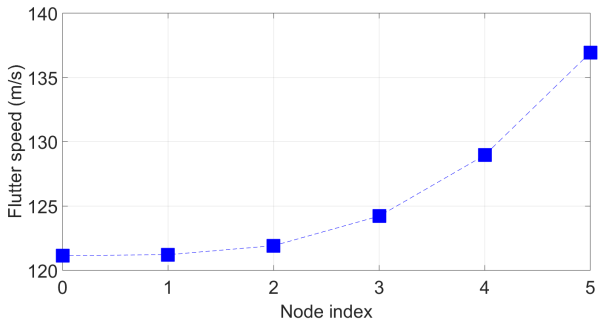

Fig. 8. Flutter speed for pinning to node n_i

$$G = \begin{bmatrix} 0 & 0 & 0 & 0 & 0 \\ 0 & 0 & 0 & 0 & 0 \\ 0 & 0 & 0 & 0 & 0 \\ 0 & 0 & 0 & 0 & 0 \\ 0 & 0 & 0 & 0 & 1 \end{bmatrix} \tag{14}$$

A. Frequency-domain analysis

The Bode magnitude graph for speed 100 m/s of the flexible wing without control and with cooperative state feedback is in Figure 9. Significant changes in modes damping can be observed. The first two modes are damped more than 7dB.

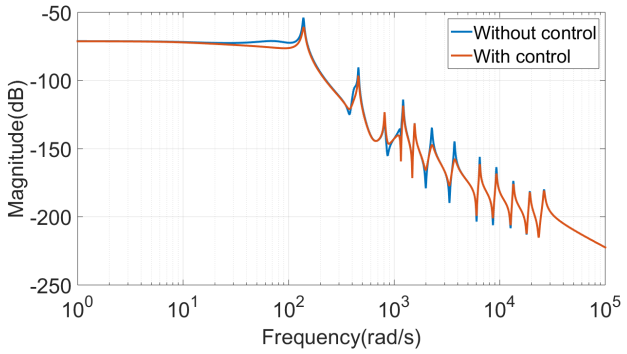

Fig. 9. Magnitude Bode plot for 100 m/s

B. Time-domain analysis

In a time-domain analysis, gust response is considered. The model of a gust is well-known function

$$H_{gust}[1 - \cos(2\pi \frac{1}{T_{gust}})].$$

Figures 10 and 12 show responses of all five nodes for speed 100m/s (below the flutter speed). Higher damping of a system with the controller can be seen. Responses above the flutter speed are captured in Figures 11 and 13, where the system without control is unstable.

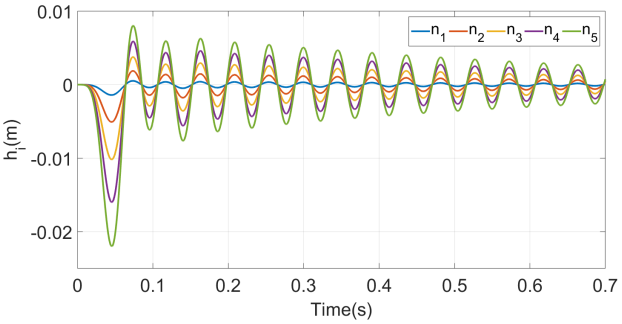

Fig. 10. Gust response 100 m/s – System without controller

V. CONCLUSIONS

An aeroelastic wing model inspired by morphing wing aircraft concept was introduced. The whole dynamics of a wing has been split into several wing segments and represented as a group of agents. The dynamical model has been used for controller design. Active flutter suppression is formulated as a state synchronization in a network of identical LTI systems. We have shown controllers damping capabilities and flutter speed dependence on pinning matrix.

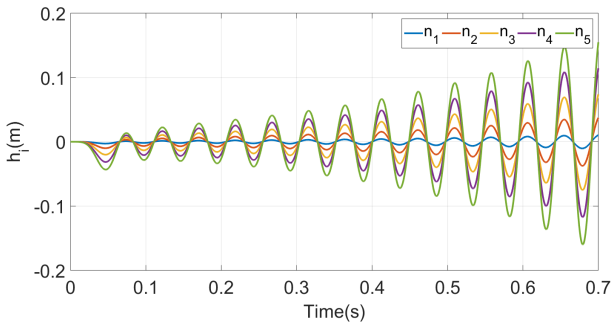

Fig. 11. Gust response 140 m/s – System without controller

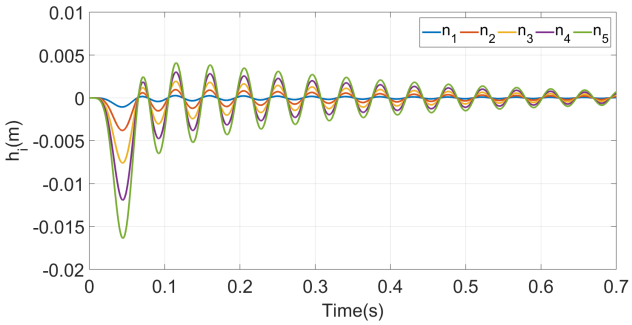

Fig. 12. Gust response 100 m/s – System with controller

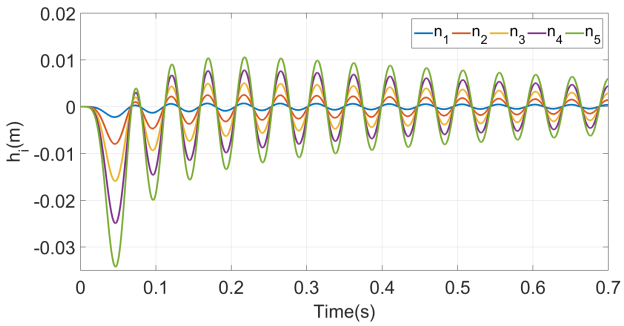

Fig. 13. Gust response 140 m/s – System with controller

REFERENCES

[1] I. E. Garrick and W. H. Reed, "Historical development of aircraft flutter," *Journal of Aircraft*, vol. 18, pp. 897–912, 1981.

[2] T. A. Weisshaar, "Morphing aircraft systems: Historical perspectives and future challenges," *Journal of Aircraft*, vol. 50, pp. 337–353, 2013.

[3] A. Y. N. Sofla, S. A. Meguid, K. T. Tan, and W. K. Yeo, "Shape morphing of aircraft wing: Status and challenges," *Materials and Design*, vol. 31, pp. 1284–1292, 2010.

[4] G. P. Tandon, A. J. W. McClung, and J. W. Baur, *Shape Memory Polymers for Aerospace Applications: Novel Synthesis, Modeling, Characterization and Design*. DEStech Publications, Inc., 2016.

[5] J. Hetrick, R. Osborn, S. Kota, P. Flick, and D. Paul, "Flight testing of mission adaptive compliant wing," in *48th AIAA/ASME/ASCE/AHS/ASC Structures, Structural Dynamics, and Materials Conference*, 2007.

[6] R. Olfati-Saber, J. A. Fax, and R. M. Murray, "Consensus and cooperation in networked multi-agent systems," *Proceedings of the IEEE*, vol. 95, pp. 215–233, 2007.

[7] Y. Hong, J. Hu, and L. Gao, "Tracking control for multi-agent

consensus with an active leader and variable topology," *Automatica*, vol. 42, pp. 1177–1182, 2006.
[8] X. Li, X. Wang, and G. Chen, "Pinning a complex dynamical network to its equilibrium," *IEEE Trans. Circuits syst. I*, vol. 51, pp. 2074–2087, 2004.
[9] X. Wang and G. Chen, "Pinning control of scale-free dynamical networks," *Physica A*, vol. 310, pp. 521–531, 2002.
[10] A. Kotikalpudi, H. Pfifer, and G. J. Balas, "Unsteady aerodynamics modeling for a flexible unmanned air vehicle," in *AIAA Atmospheric Flight Mechanics Conference, AIAA AVIATION Forum*, 2015.
[11] G. P. Guruswamy, "Integrated approach for active coupling of structures and fluids," *AIAA Journal*, vol. 27, pp. 788–793, 1989.
[12] ——, "Computational-fluid-dynamics- and computational-structural-dynamics-based time-accurate aeroelasticity of helicopter rotor blades," *Journal of Aircraft*, vol. 47, pp. 858–863, 2010.
[13] E. Albano and W. P. Rodden, "A doublet-lattice method for calculating lift distributions on oscillating surfaces in subsonic flows," *AIAA Journal*, vol. 7, pp. 279–285, 1969.
[14] P. Konstadinopoulos, D. F. Thrasher, D. T. Mook, A. H. Nayfeh, and L. Watson, "A vortex-lattice method for general, unsteady aerodynamics," *Journal of Aircraft*, vol. 22, pp. 43–49, 1984.
[15] J. R. Wright and J. E. Cooper, *Introduction to Aircraft Aeroelasticity and Loads, 2nd Edition*. Willey, 2015.
[16] T. Theodorsen, "General theory of aerodynamic instability and the mechanism of flutter," NASA Center for AeroSpace Information, Langley Research Center, Hampton, Virginia 23681-2199, Tech. Rep., January 1949.